Vol. 44, No. 1 (2022) 143-149, DOI: 10.24874/ti.1144.06.21.08

Tribology in Industry

www.tribology.rs

RESEARCH

Locally Resolved Residual Stress Measurements in (Al,Ti)N Coatings Using Raman Spectroscopy

Bernd Breidenstein[a], Nils Vogel[a,*], Harald Behrens[b], Marcel Dietrich[b], Jon M. Andersson[c]

[a]*Leibniz University Hannover, Institute of Production Engineering and Machine Tools, An der Universität 2, 30823 Garbsen, Germany,*
[b]*Leibniz University Hannover, Institute for Mineralogy, Callinstr. 3, 30167 Hannover, Germany,*
[c]*Seco Tools AB, Björnbacksvägen 2, 73782 Fagersta, Sweden.*

Keywords:

Residual stress
PVD
Coating
Raman-spectroscopy
Titanium aluminum nitride
X-ray diffraction

* Corresponding author:

Nils Vogel
E-mail: vogel@ifw.uni-hannover.de

Received: 22 June 2021
Revised: 9 June 2021
Accepted: 29 August 2021

A B S T R A C T

The residual stress state in tool coatings can positively influence tool life. Measurement in strongly curved surfaces e.g. in the cutting edge area is only possible to a limited extent by means of X-ray diffraction (XRD). Raman spectroscopy offers great potential for determining the residual stress state in this area. Therefore, the aim is to determine the fundamental limits of residual stress measurement by XRD on coated carbide tools and to determine and evaluate the suitability of Raman spectroscopy. On typical cutting tools only a small area on the rake face can provide reliable measurement results using conventional XRD methods. Using the XRD results as reference, Raman spectroscopy shows plausible results for residual stresses induced into the coating by mechanical or thermal post-treatment. Coating-induced residual stresses cannot be reliably detected because other coating properties are also changed by modified coating processes that induce higher compressive residual stresses.

1. INTRODUCTION

The effect of thin hard material coatings on the service life of cutting tools has been subject to numerous investigations. The coating of tools gives them tribological, thermal and mechanical properties, which cannot be achieved either by the tool or the coating material alone. Coatings produced by physical vapour deposition (PVD) processes exhibit a residual stress distribution strongly influenced by the coating parameters like the bias voltage [1]. Similar to fatigue stressed components, compressive residual stresses tend to have a positive influence on service life and thus on the performance of cutting tools [2–5]. This behavior can also be observed for coatings if, for example, the mechanical post-treatment by blasting is considered, which increases compressive residual stresses in the coating [2]. However, the tool life can only be increased up to a global compressive residual stress maximum, afterwards the tool life decreases with increasing compressive residual stresses [6].

In this work, residual stresses were measured using the XRD $\sin^2\psi$-method. A prerequisite for using this method is amongst other things a flat surface. Residual stresses on surfaces with a more complex geometry cannot be determined reliably with this method. This is also the reason why residual stresses cannot be measured directly in the cutting edges, which have radii between r_β = 5 µm and 100 µm. However, due to its thermal, tribological and mechanical loads, the cutting edge has proven to be a weak point for coated tools and offers large potential for optimizing tool life [7]. The usual measuring surface area of a few mm^2 prevents a spatially resolved XRD measurement. A reduction of the diameter of the X-ray collimator is accompanied by a squared decrease of the intensity of the scattered radiation and thus cannot deliver statistically secured measurement data in a reasonable measurement time [8]. Raman spectroscopy offers a high potential for a residual stress measurement in Raman-active samples such as (Al,Ti)N coatings [9-11]. The laser beam with a diameter of a few µm penetrates into the material and is therefore suitable for locally- and depth-resolved measurements. The sample to be examined is irradiated with monochromatic light and the incoherently backscattered light is analysed. High intensities and a high local resolution of a few micrometers can be achieved (see Fig. 1 for comparison of X-ray collimator and Raman spot diameters).

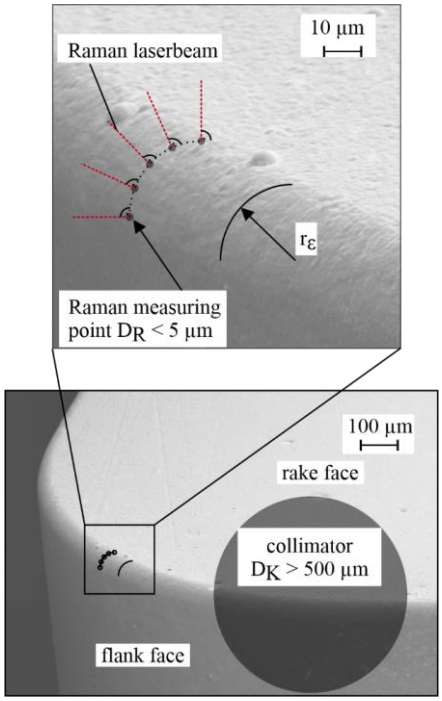

Fig. 1. Comparison of the measuring spot sizes of X-ray diffraction and Raman spectroscopy

In order to obtain optimal measuring conditions, the laser beam must be aligned perpendicular to the measured surface. The aim of this study is to determine the geometric limits of residual stress measurements by XRD on tools and to qualify the alternative Raman spectroscopy for residual stress measurements on the rake face of coated carbide tools.

2. EXPERIMENTAL DETAILS

2.1 Tool details and coating process

For the investigations, inserts with five different production-related residual stress conditions were investigated. These were carbide inserts with the geometry SNMA120408 containing 94 wt % WC and 6 wt % Co covered by a PVD monolayer-coating of (Al,Ti)N. For the first three samples, the residual stress state was influenced only by the coating process. Different bias voltages (U_B = -25, -35, -65 V) provide different residual stress states in the tool coating. Some of the tools that were processed with U_B = -65 V were heat-treated for stress-relief annealing. For this purpose, the tools were annealed to 800 °C for one hour in an argon atmosphere. Tools that were coated with U_B = -35 V were additionally wet-blasted in order to increase the compressive residual stress. Edged Al_2O_3 media with an average grain size of about 60 µm was used as abrasive and added to a water based slurry. An air pressure of 3 bar was applied to accelerate the slurry towards the inserts. The strain-free lattice spacing d_0 was determined by X-ray diffraction in the strain-free direction.

2.2 Residual stress measurement

In order to determine the residual stress state in the coatings, the $\sin^2\psi$ method was applied in the first step on two samples for each coating parameter, and five positions on the rake face were analysed [12]. These measurements were performed with a SEIFERT five-circle diffractometer system, XRD 3003 ETA from GE Inspection Technologies. It is equipped with a GE SZ20/SE scintillation counter. CoKα radiation and a point collimator with a diameter of 2 mm were used. Subsequently, in order to evaluate the homogeneity of the residual stresses of non-treated tools (U_B = -65 V), a mapping was performed on the rake face. Due to the small spot size Raman measurements may be affected by local variations in the coating

composition. In order to exclude such effects, the ratio of aluminium to titanium was analysed using energy-dispersive X-ray spectroscopy (EDX) measurements on the rake face of the tools.

2.3 Raman spectroscopy

For the Raman measurements the described tools with the same coating parameters have been selected. All Raman spectra were recorded using a Bruker Senterra Micro Raman equipped with an Olympus BX51 microscope. All samples were analysed in the exact middle of the rake face. For excitation a 532 nm laser was used. Spectra were recorded with 2 mW using 100 x magnification, which results in a lateral laser spot size of about 1 µm in diameter. The Raman spectrum of the (Al,Ti)N coated tools (U_B = -65 V / r_β = 50 µm / untreated) is shown in Fig. 2. The most intensive peak around 250 cm^{-1} represents the transversal (perpendicular to the wave) acoustic / longitudinal (parallel to the wave) acoustic mode TA/LA [9].

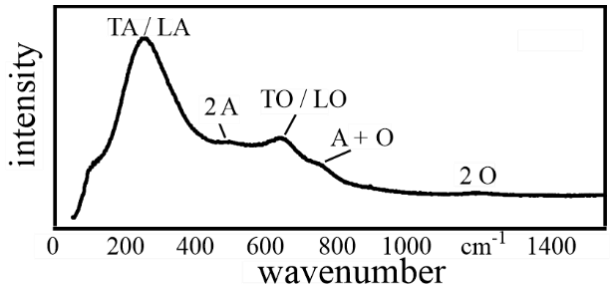

Fig. 2. Optical /acoustic modes in the (Al,Ti)N spectrum, exemplary sample (U_B = -65V, r_β = 50 µm).

Towards higher wave numbers a triplet of signals arises. The second order acoustic mode 2A around 475 cm^{-1}, the transversal optical / longitudinal optical mode TO/LO around 650 cm^{-1} and the acoustic and optical mode A+O around 750 cm^{-1}. The very weak and broad signal around 1200 cm^{-1} represents the second order optical mode 2O [9].

3. RESULTS

3.1 Residual stress ($sin^2\psi$)

The XRD residual stress measurements by $sin^2\psi$ method show a clear dependence on the coating parameter U_B (Fig. 3). A low bias voltage of U_B = -25 V leads to the lowest compressive residual stress state of σ = -710 ± 114 MPa.

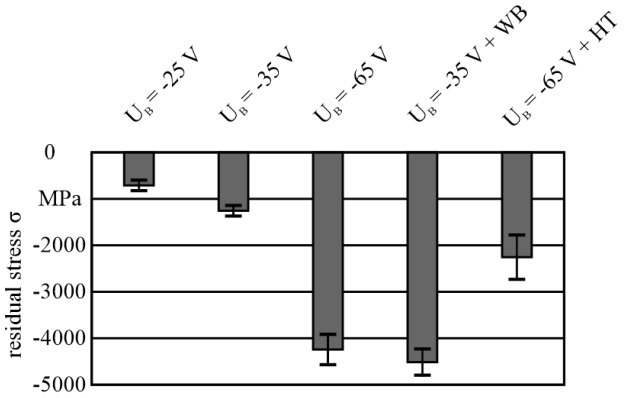

Fig. 3. Coating residual stresses at different bias-voltages and after post-treatment.

With increasing bias voltage, the compressive residual stress also increases up to σ = -4240 ± 327 MPa at U_B = -65V. Considering the tool that was coated with a bias voltage of U_B = -35 V and then wet-blasted, an increase of the compressive residual stresses from σ = -1260 ± 124 MPa in the unblasted state to σ = -4510 ± 285 MPa after post-treatment is observed. This shows that a higher residual stress state can be achieved by post-treatment than with a significantly higher bias voltage. The heat treated tools, which initially had coating induced residual stresses of σ = -4240 ± 327 MPa, showed a significantly lower residual stress of σ = -2250 ± 478 MPa after heat treatment at 800° C for 1 h in Ar-atmosphere.

3.2. Homogeneity of residual stresses

To assess the homogeneity of the residual stresses in the coating, 49 measurements (7 x 7) were carried out on the rake face using the $sin^2\psi$-method (Fig. 4). Especially next to the cutting edge the measurements showed a wide scattering of the results. It is assumed that these strong variations near the edge are caused by unfulfilled ideal diffraction conditions. To investigate this behavior in detail, the tool was rotated by 180° around the z-axis for the repeat measurement. Afterwards, the difference between the two measurements was determined as shown in Fig. 4. It can be seen here that high differences between both measurements occur near the cutting edge. Since both measurements were taken at the same positions, it is expected that the strong deviations occur due to the already mentioned invalid ideal diffraction conditions (edge effects). It can be clearly seen that the distance between the measuring position and the cutting edge has a great influence on the validity of the measurement results.

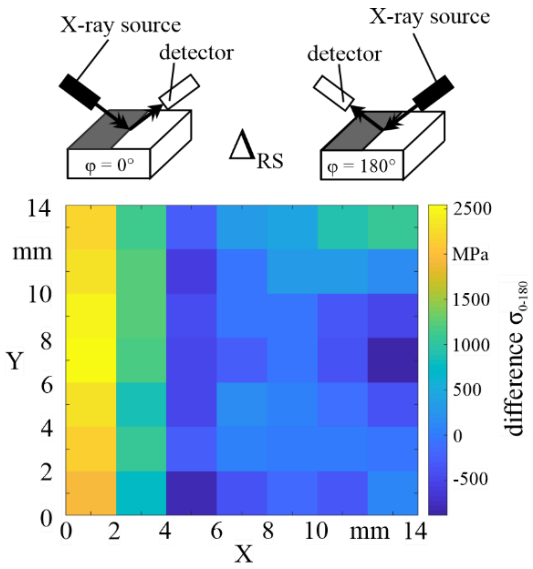

Fig. 4. Difference between the residual stress measurement results at two azimuth angles of φ = 0° and φ = 180° (U_B = -65 V).

In order to determine the distance to the cutting edge from which a reliable result can be obtained, measurements were taken at distances d from the cutting edge of 0; 0.5; 1.5; 2.5; 3.5; 4.5 mm with φ = 0, 90, 180, 270 °. Coatings have an isotropic residual stress state, so it is expected that all measurements will deliver similar results. However, noticeable deviations between the four different sample orientations are evident (Fig. 5). Furthermore, for each orientation variations are particularly pronounced near the edge, and the curve flattens from a distance from the edge of 2.5 mm. As a result, this is the minimal distance to get reliable results for the residual stress determination using XRD with this setup. In reference to the square tool with an edge length of 12.7 mm, there is a measurable area of 7.7 x 7.7 mm in the centre of the insert.

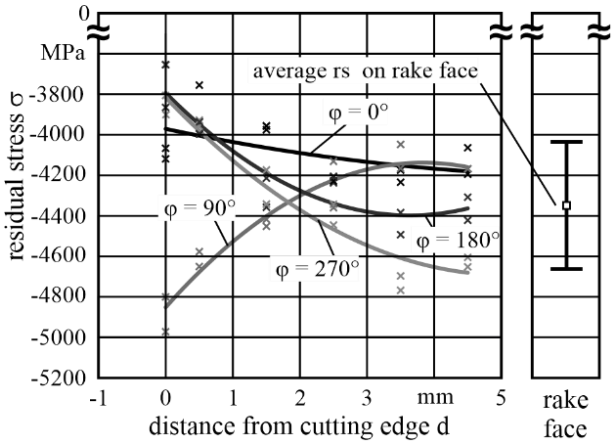

Fig. 5. Differences of the residual stress values determined by XRD with varied distances to the cutting edge (U_B = -65 V).

3.3 Coating Composition

All tools have a very similar coating composition of $Al_{56}Ti_{44}N$. The deviation from the mean value is less than 1 at % composition (Al 55,74 ± 0,52 at % / Ti 44,26 ± 0,52 at %). Neither the different bias voltages nor the post-treatment processes have any influence on the coating composition. This indicates that an influence on the Raman spectrum by a different coating composition can be excluded [11].

3.4 Raman Measurements

The Raman measurement basically delivers a spectrum as shown in Fig. 2. In the context of these investigations, only the stress induced peak shift of the transversal optical/longitudinal optical mode (TO/LO) is relevant for the determination of the residual stress [10]. Hence only the range between 500 and 800 cm^{-1} is considered in this study (Fig. 6).

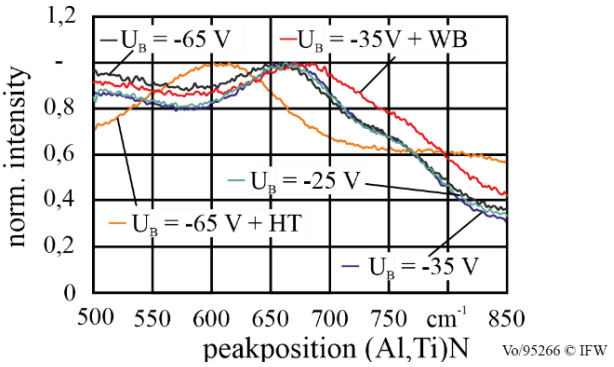

Fig. 6. Raman spectra of the five samples in the stress-related range measured on the rake face.

For better comparison the spectra were normalized to the highest point within this region. Spectra of the tools without post-treatment, which were coated with a bias voltage of 25, 35 and 65 V, do not differ much in their peak position P of approximately 650 – 670 cm^{-1}. A minor trend of a peak shift towards lower wave numbers with increasing bias voltages can be seen (Fig. 6). To determine these peak shifts more precisely, each spectrum was fitted in the area of interest (typically between 610 – 710 ± 20 cm^{-1} depending on peak shape) using a simple Gaussian function. This gives a reproducible peak position with low standard deviation (Fig. 7). It is also clear here that the mechanically and thermally post-treated coatings differ significantly from the untreated coatings.

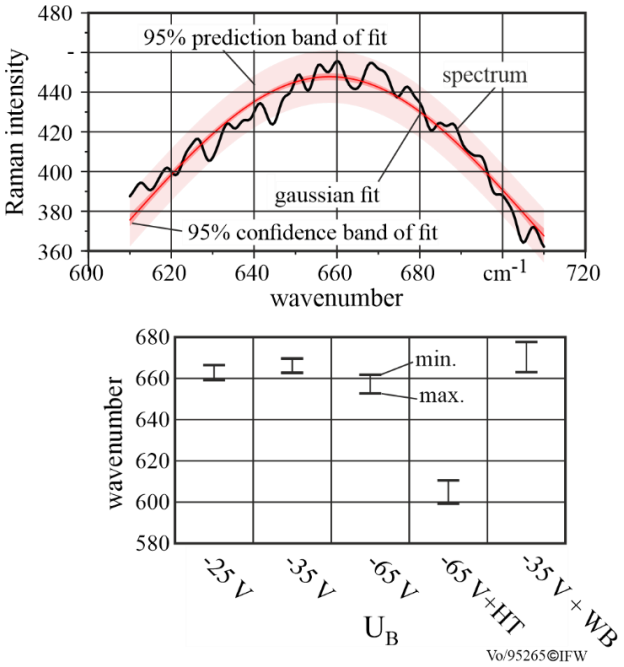

Fig. 7. Exemplary fit procedure (top) and variation range of Raman measurements (bottom).

4. DISCUSSION

The X-ray analysis of the residual stresses shows that different residual stress states can be reached by different bias voltages. For the investigated process parameters the residual stress varies from about -700 MPa to about -4200 MPa with a change in bias voltage from -25 to -65 V. These initial investigations have shown similar behaviour to Ahlgren et al. [1] and provide different residual stress states as a basis for further analysis by Raman spectroscopy. A post-treatment by means of a wet blasting process allows an increase of compressive residual stresses independent of the coating process. Blasting processes are actually used for chemical vapor deposition (CVD) coatings that have tensile residual stresses induced by coating processes [13,14]. In our case it is interesting to note that a compressive residual stress state already induced by the coating process can be significantly increased further by the blasting process. A reduction of the residual stress is possible by heat treatment. This can be explained by a classic stress-relief annealing of the coating. The grid residual stress measurement in order to evaluate the homogeneity of the residual stresses has shown that the measured residual stress state in the centre of the rake face can be regarded as homogeneous, whereas the results scatter towards the edges of the tool. This can be explained by edge effects, which are caused by the non-ideal diffraction conditions at the edge as described above and is probably not caused by different residual stresses in the coating. The problem is that the size of the X-ray spot (collimator diameter 2 mm, circular profile) is getting larger by its projection to the specimen surface (Fig. 8). At the Bragg angle of $\theta = 25\,°$ the spot becomes elliptical, and at different inclination angles ψ with $-45\,° < \psi < 45\,°$ the ellipse becomes longer and gets diagonal. This projected X-ray spot becomes longer than the specimen surface and may lead to misinterpretations of the measured peaks. A measurement close to the cutting edge on a flat surface therefore does not provide reliable results.

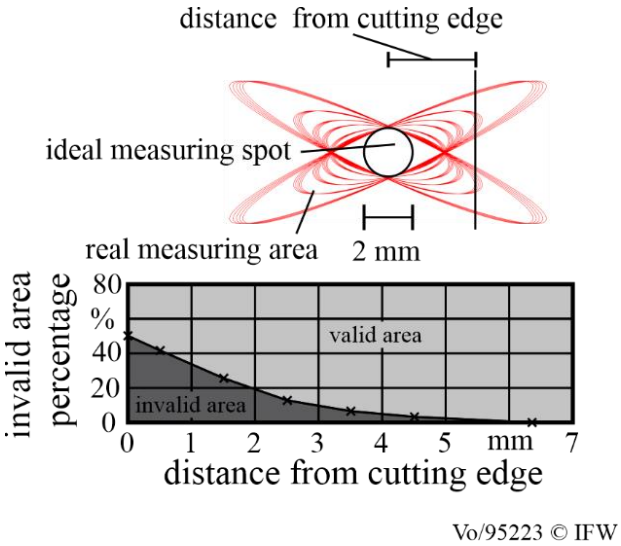

Fig. 8. Validity of the measuring area next to the cutting edge.

The results from the Raman measurements show that the residual stress states induced by wet blasting or heat treatment can be identified reliably. This means that tools with different residual stresses can be distinguished by Raman spectroscopy. With increasing compressive residual stresses due to wet blasting, the Raman peak position shifts to higher wave numbers. If the residual stress state is reduced by annealing, a peak shift to lower wave numbers occurs. This shift is in line with studies for the cutting materials cubic boron nitride and polycrystalline diamond [15,16].

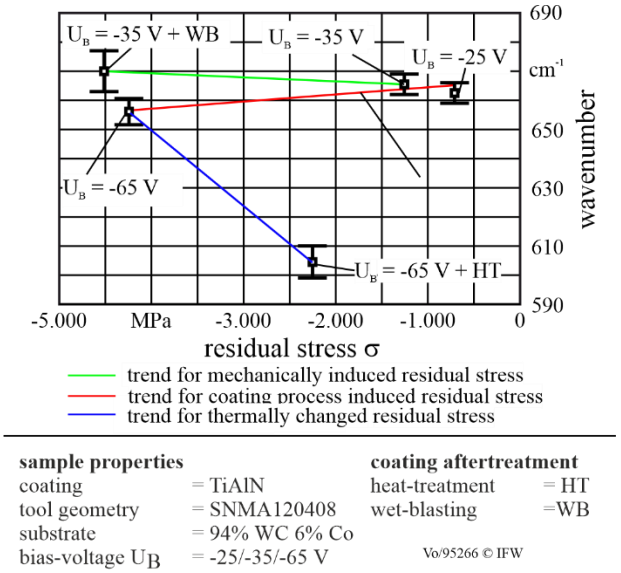

Fig. 9. Influence of coating process and post-treatment on Raman peak position.

However, as Fig. 9 shows, the corresponding trend is not detectable in tools with coating process-induced residual stresses. On the contrary, the trend is reversed, so that the peak position shifts slightly to lower wave numbers with increasing residual stress. The shift to lower wave numbers with increasing coating induced residual stresses has not been observed previously and indicates that a change in the bias voltage not only changes the residual stress state, but also other coating properties that interfere with the residual stress effect in the Raman spectrum. It is known from the PVD coating with titanium nitride that the crystal lattice is expanded with increasing bias voltage [17]. The reason is argon or nitride ions which are entrapped in the TiN-crystal. This counteracts compression of the lattice by compressive residual stresses.

In the present investigations no argon was used for the coating of the tools, but an entrapment of nitrogen ions would be possible. An increase of the strain-free lattice spacing caused by ion bombardment induced defects has been observed previously for arc deposited TiAlN coatings [17] and a similar effect might be present also in the present tools. The measured strain-free lattice spacings by XRD confirms this hypothesis, as shown in Fig. 10; an increasing bias voltage also increases the strain-free lattice spacing d_0. The position of the peak in the Raman spectrum depends on the length of the atomic bonds. If interstitial atoms are introduced, the crystal lattice expands, d_0 increases, the length of the atomic bonds increases and the peak position shifts to lower wavenumbers [18]. However, this leads to an increase in the compressive residual stresses determined by X-ray. It should be noted that the determination of residual stresses using the angle-dispersive XRD method works independently of d_0 [19]. It can thus be stated that residual stress measurements by Raman spectroscopy are not possible if the crystal lattice structure varies. If no additional interstitial atoms are present, as in the case of mechanical post-treatment, the atomic bonds shorten due to higher compressive residual stresses and the peak shifts to higher wavenumbers, as can be seen at U_B = -35 V and U_B = -35 V + WB.

It is also evident that heat treatment reverses this increase in the lattice spacing, due to partial healing out of defects, and that wet blasting has no significant effect on the strain-free lattice spacing. This means that the shift of the Raman peak for the heat treated sample is likely due to a combination of relaxed stress and decreased strain free lattice spacing, whereas the shift for the wet blasted sample is caused mainly by increased compressive stress.

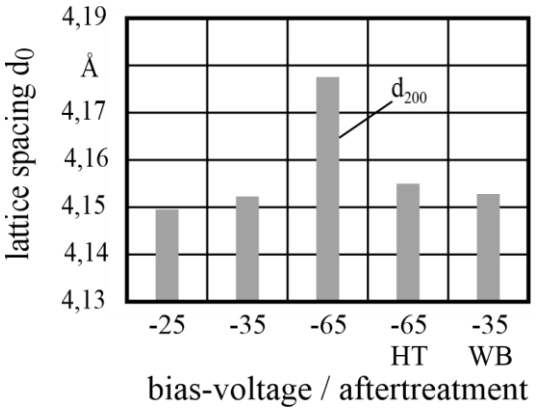

Fig. 10. Strain-free lattice spacing in coatings produced with different bias voltages and post-treatments.

The constant coating composition of the different tools also excludes an influence of chemical composition on the Raman peak position [9].

5. CONCLUSION

On the one hand, the investigations have shown that the classical XRD methods do not provide reliable results for the determination of residual stresses close to the cutting edge. On the other hand, measurements using Raman spectroscopy of (Al,Ti)N coatings have shown that mechanically or thermally altered residual stresses can be detected. This enables local stress distributions to be evaluated at a resolution of down to about 1 µm, for

example at the cutting edge of an insert. However, coating process (bias voltage) induced residual stresses cannot yet be reliably detected because not only the residual stress, but also the strain-free lattice spacing changes in dependency of the bias voltage. The separation of these two effects would enable an even more powerful application of Raman spectroscopy for local stress investigations, and will be a task for future investigations.

Acknowledgement

The research project BR 2967/11-1 BE1720/41-1 "Effects of cutting edge residual stresses on the wear behavior of PVD-coated cutting tools" is funded by the German Research Foundation (DFG)

REFERENCES

[1] M. Ahlgren, H. Blomqvist, *Influence of bias variation on residual stress and texture in TiAlN PVD coatings*, Surface and Coatings Technology vol. 200, iss. 1-4 pp. 157–160, 2005, doi: 10.1016/j.surfcoat.2005.02.078

[2] F. Klocke, T. Schroeder, E. Bouzakis, A. Klein, *Manipulation of coating and subsurface properties in reconditioning of WC–Co carbide cutting tools*, Surface & Coatings Technology vol. 202, iss. 4-7 pp. 1194–1198, 2010, doi: 10.1016/j.surfcoat.2007.06.023

[3] B. Denkena, B. Breidenstein, *Residual Stress Distribution in PVD-Coated Carbide Cutting Tools – Origin of Cohesive Damage,* Tribology in Industry, vol. 34, no. 3, pp. 158-165, 2012.

[4] B. Breidenstein, *Surfaces and subsurface of highly stressed components,* post-doctoral lecturer qualification, Leibniz Universität Hannover, 2011. (in German)

[5] G. Skordaris, K.D. Bouzakis, T. Kotsanis, P. Charalampous, E. Bouzakis, B. Breidenstein, B. Bergmann, B. Denkena, *Effect of PVD film's residual stresses on their mechanical properties, brittleness, adhesion and cutting performance of coated tools*, CIRP Journal of Manufacturing Science and Technology vol. 18, pp. 145–151, 2017, doi: 10.1016/j.cirpj.2016.11.003

[6] F. Klocke, C. Gorgels, A. Stuckenberg, E. Bouzakis, *Qualification of Coatings to Predict Wear Behavior of Micro Blasted Cutting Tools*, Key Engineering Materials vol. 438, pp 23-29, 2010, doi: 10.4028/www.scientific.net/KEM.438.23

[7] B. Denkena, D. Biermann, *Cutting edge geometries*, CIRP Annals, vol. 63, iss. 2, pp. 631–653, 2014, doi: 10.1016/j.cirp.2014.05.009

[8] J.M. Plöger, *Influencing the subsurface by high-speed turning*, PhD thesis, Leibniz Universität Hannover, 2002. (in German)

[9] C.P. Constable, J. Yarwood, W.-D. Münz, *Raman microscopic studies of PVD hard coatings,* Surface and Coatings Technology, vol. 116-119, pp. 155–159, 1999, doi 10.1016/S0257-8972(99)00072-9

[10] C.P. Constable, D.B. Lewis, J. Yarwood, W.-D. Münz, *Raman microscopic studies of residual and applied stress in PVD hard ceramic coatings and correlation with X-ray diffraction (XRD) measurements,* Surface and Coatings Technology, vol. 184, iss. 2-3 pp. 291–297, 2004, doi: 10.1016/j.surfcoat.2003.10.014

[11] H.C. Barshilia, K.S. Rajam, *Raman spectroscopy studies on the thermal stability of TiN, CrN, TiAlN coatings and nanolayered TiN/CrN, TiAlN/CrN multilayer coatings*, Journal of Materials Research. vol. 19, iss. 11, pp. 3196–3205, 2004, doi: 10.1557/JMR.2004.0444

[12] E. Macherauch, P. Müller, *The $\sin^2\psi$ method of XRD residual stress measurement,* Zeitschrift für angewandte Physik, vol. 13, pp. 305-312, 1961. (in German)

[13] E. Bouzakis, *Performance Enhancement of PVD Coated Cemented Carbeide Tools by Blasting,* PhD thesis, Technische Hochschule Aachen, 2008. (in German).

[14] M. Tkadletz, J. Keckes, N. Schalk, I. Krajinovic, M. Burghammer, C. Czettl, C. Mitterer, *Residual stress gradients in α-Al_2O_3 hard coatings determined by pencil-beam X-ray nanodiffraction: The influence of blasting media,* Surface & Coatings Technology, vol. 262, pp. 134-140, 2015, doi: 10.1016/j.surfcoat.2014.12.028

[15] J.A. Sanjurjo, E. Lopez-Cruz, P. Vogl, M. Cardona, *Dependence on volume of the phonon frequencies and their effective charges of several III-V semiconductors*, Physical Review B, vol. 28, iss. 8-15, pp. 4579–4584, 1983, doi: 10.1103/PhysRevB.28.4579

[16] S.A. Catledge, Y.K. Vohra, R. Ladi, R. Ghanshyam, *Micro-Raman stress investigations and X-ray diffraction analysis of polycrystalline diamond (PCD) tools*, Diamond and Related Materials vol. 5, iss. 10 pp. 1159–1165, 1996, doi: 10.1016/0925- 9635(96)00534-1

[17] J.M. Andersson, J. Vetter, J. Müller, J. Sjölén, *Structural effects of energy input during growth of Ti1 – xAlxN (0.55 ≤ x ≤ 0.66) coatings by cathodic arc evaporation,* Surface and Coating Technology, vol. 240, pp. 211-230, 2014, doi: 10.1016/j.surfcoat.2013.12.018

[18] D. Tuschel, *Stress, Strain and Raman Spectroscopy*, Spectroscopy, vol. 14, iss. 9, pp. 10-21 2019.

[19] L.Spieß, G. Teichert, R. Schwarzer, H. Behnken, C. Genzel, *Modern X-ray diffraction* Wiesbaden: Vieweg+Teubner 2009. (in German)